SUPPLEMENTARY INFORMATION

Supplementary Methods:

Isolation of primary mammary tumor organoids

Organoids were isolated from primary mammary tumors by mechanical and enzymatic digestion using collagenase (C2139; Sigma-Aldrich) and trypsin (27250-018; Gibco Life Technologies), as previously described (28,29). In brief, tumors were harvested from 8- to 15-wk-old mice, minced with a scalpel, and digested for 1 h at 37°C in collagenase solution: DMEM/F12 (10565-018; Gibco Life Technologies) with 2 mg/mL collagenase (C2139, Sigma-Aldrich), 2 mg/mL trypsin (27250-018; Gibco LifeTechnologies), 5% (vol/vol) FBS (F0926; Sigma-Aldrich), 5 μg/mL insulin (I9278; Sigma-Aldrich), and 50 μg/mL gentamicin (15750; Gibco Life Technologies). The suspension was centrifuged at 1500 rpm for 10 min to remove cellular debris, and the pellet was treated with 2 U/μL DNase (D4263; Sigma-Aldrich). Tumor organoids were separated from single cells by differential centrifugation at 1500 rpm for 10 seconds. Organoids with 100-200 cells were obtained by differential centrifugation at a lower speed, 600 rpm for 3 seconds. For control experiments, tumor organoids were embedded in 7 mg/mL rat tail collagen-I (354249, Corning) gels at 2-3 organoids/μL as 150 μL suspensions and plated in a 24-well multiwell glass bottom plate (662892; Greiner Bio-One). Each well was cultured with “organoid media”: DMEM/F12 (10565-018, Gibco), 1% v/v insulin, transferrin, selenium (51500, ThermoFisher) and 1% v/v penicillin/streptomycin (15140-122, Gibco) supplemented with 2.5 nM FGF2 (F0291, Sigma).

Immunofluorescence staining

Murine primary tumors were collected, fixed, and stained as previously described (6). OCT blocks from both murine and human tumors were sectioned at 30 μm thickness using a Leica cryostat (Leica Biosystems) set to −27 °C. Sections were placed on Superfrost Plus Gold microscope slides (15-188-48; Fisherbrand) and stored at -80°C. For antibody staining, slides were thawed at ambient temperature, rinsed twice with PBS to remove OCT and permeabilized with 0.5% Triton X-100 for 1 h. Samples were then blocked with 10% FBS / 1% BSA / 0.2% Triton X-100 in D-PBS for 2-3 h and incubated

with primary antibody solution overnight at 4°C in 1% FBS / 1%BSA / 0.2% Triton X-100 in D-PBS. Slides were then rinsed three times in D-PBS and incubated with secondary antibodies diluted in D-PBS with 1%FBS / 1% BSA / 0.2% Triton X-100 for 4 h at ambient temperature. Slides were rinsed three times in D-PBS for 10 min. Slides were mounted using Fluoromount Aqueous Mounted Medium (Sigma; F4680) and covered with rectangular #1.5 High Precision 24x50 mm, 170 μm-thick Microscope Cover Glasses (Thor Labs; CG15KH). Immunofluorescence staining was done in at least three biological replicates. Rabbit anti-CD31 (Abcam; ab28364; 1:100) and collagen IV (Millipore; AB769; 1:10) were used as primary antibodies. Goat anti-rabbit AlexaFluor 647 (ThermoFisher; A32733; 1:200) was used as secondary antibody. Nuclei were stained with DAPI (Roche; 10236276001; 1:1000). Entire image scans (16 μm total tissue depth, in 1 μm z-steps) were manually scored by two independent researchers based on 2D and 3D optical reconstructions. Discordant scores between the two observers were not used. Microvessels were considered for analysis if they intersected the tissue section with an approximately circular cross-section. Mosaic vessels were defined by the presence of tumor cells in apparent contact with the vessel lumen in 2D and 3D, with an absence of CD31 and collagen IV staining.

To conduct immunofluorescence staining within microvessel devices, the vessels were washed with PBS for 5 min, fixed with 3.7% paraformaldehyde (Sigma) for 15 min, permeabilized with 0.1% Triton X-100 (Sigma) for 15 min, and blocked with 10% FBS overnight at 4 °C. Microvessels were incubated overnight at 4 °C with anti-β-catenin (E-5) primary antibody (Santa Cruz, sc-7963,1:300) and for 20 min at ambient temperature with goat anti-mouse IgG (H+L), Alexa Fluor Plus 488 (ThermoFisher Scientific, A32723, 1:100). Nuclei were stained using DAPI solution (Invitrogen, D3571, 1:1000). Confocal z-stack images were captured on a Zeiss 780 laser-scanning confocal microscope (Carl Zeiss Microscopy). To reconstruct microvessels, approximately four hundred 0.5 μm slices were acquired, using a 40X objective.

Supplementary Figure 1. Steps used to calculate permeability coefficients in 3D using perfusable microvessel models. Sample data from an experimental permeability measurement for one tracer molecule. The following equation was used to calculate permeability: $P_{3D}= (1/\Delta I_f) (dI_f/dt) (d/4)$, where ΔI_f is the initial increase in fluorescence intensity (when the vessel is being filled with the fluorescent probe), (dI_f/dt) is the rate of increase in fluorescence intensity as the solute is being transported from the vessel to the ECM, and d is the diameter of the vessel. Permeability coefficients were calculated in cm/s. The fluorescent intensity values obtained over time were divided in 3 regions: (i) the "noise region" (prior to the vessel being filled with the fluorescent probe), (ii) when the vessel is being filled with the fluorescent probe (ΔI_f), and (iii) when the fluorescent probe permeates into the ECM. Fluorescent intensity values were measured over time for the different fluorescent probes using Fiji. Once all data values were obtained, the aim was to find the relevant inflection point marking the transition where the vessel has been filled with fluorescent dye and starts diffusion towards the ECM. To identify this relevant inflection point, a polynomial equation of degree six was used to fit the data. The "noise region" was excluded from the original data to ensure a good fit of the polynomial and to properly estimate the relevant inflection point. To properly identify the noise region the following iterative approach was used. First, begins by using all data available and continues excluding data by applying the absolute value of the growth rate of the fluorescent intensity (using 1% increments). Second, following this iterative procedure, the data that was finally used to fit the polynomial was selected after the identified inflection points became stable after at least three iterations. If multiple inflection points were identified based on these criteria, the inflection point selected for analysis corresponds to the first one where the second derivative changes from negative to positive. If the relevant inflection point was not found, the data for that ROI were not used. Once the relevant inflection point was identified, ΔI_f was determined and (dI_f/dt) was calculated for all subsequent time points, using all available data and only stopping if a subsequent inflection point was found.

Supplementary Figure 1

time (min)	Fluorescence Intensity (au)
0	8939327.00
2	8857259.00
4	8789407.00
6	8892445.00
8	9658758.00
10	11915767.00
12	14682597.00
14	16396546.00
16	17109773.00
18	17469276.00
20	17683735.00
22	17990753.27
24	18262160.58
26	18516787.92
28	18743747.36
30	18961526.85
32	19198519.66
34	19427704.31
36	19651885.20
38	19880355.22
40	20103384.40
42	20310601.29
44	20527523.52
46	20726778.66
48	20935616.64
50	21158970.75
52	21351564.36
54	21588979.23
56	21810565.40
58	22016154.30
60	22254480.00

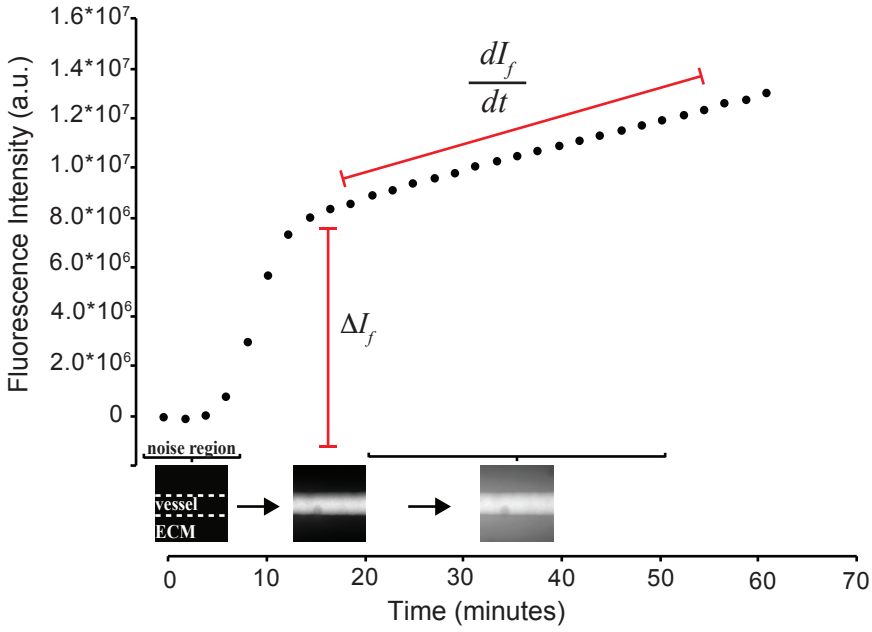

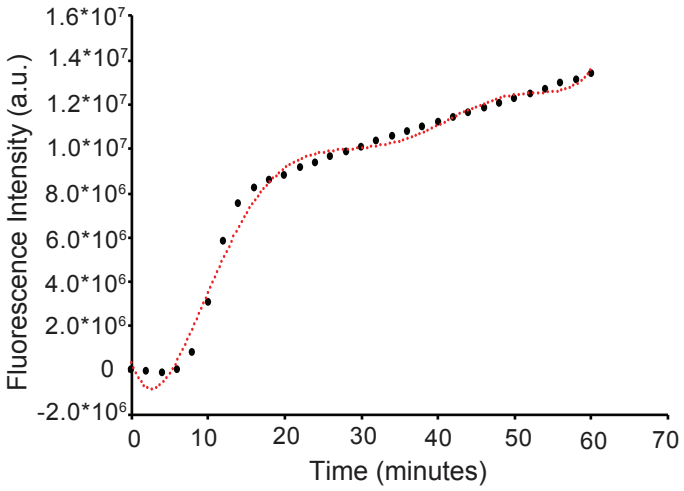

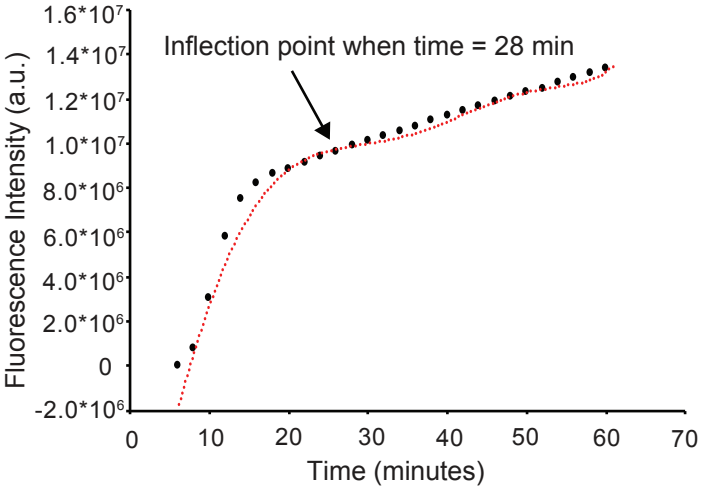

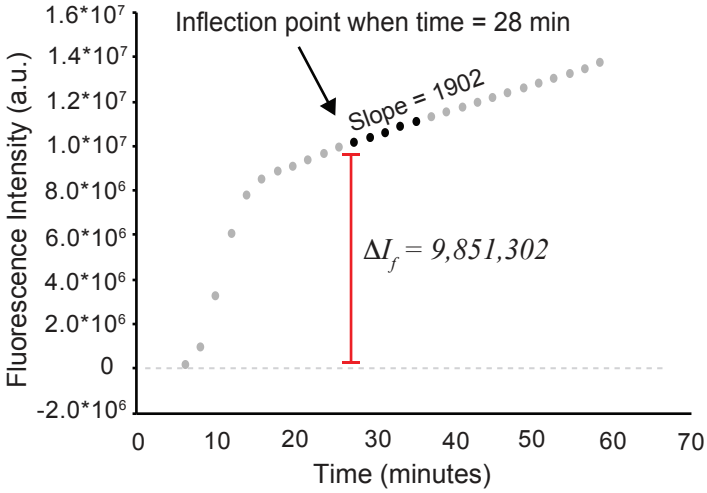

$$P_{3D} \equiv \frac{1}{\Delta I_f}\left(\frac{dI_f}{dt}\right)\frac{d}{\Delta I_f}$$

$$P_{3D} \equiv \frac{1}{9{,}851{,}302}\left(1902\right)\frac{0.02}{4}$$

$$P_{3D} \equiv 9.65*10^{-07}\ \text{cm/s}$$

Supplementary Figure 2. Mosaic vessels in primary breast tumors.

(A) Representative 3D projection of a fluorescence z-stack image of a mosaic vessel in a *ROSA^{mTmG}; MMTV-PyMT* tumor at early stages of tumor development stained with CD31 (green), collagen IV (white) and DAPI. Arrowheads mark regions lacking detectable CD31 and collagen IV immunoreactivity. Scale bar: 20 μm (B) Representative 3D projection of a fully lined vessel stained with CD31 (green), collagen IV (white) and DAPI. Scale bar: 10 μm. (C-D) Representative 2D projections and (C'-D') 3D projections of fluorescence z-stack images of a mosaic vessel in a *ROSA^{mTmG}; MMTV-PyMT* at early stages of tumor development stained with CD31 (green) and DAPI. Arrowheads mark a region lacking detectable CD31 immunoreactivity. Scale bar: 20 μm. (E-F) Representative 2D projection and (E'-F') 3D projection of fluorescence z-stack images of mosaic vessels in human breast cancer tumor stained with actin (red), CD31 (green) and DAPI. Arrowheads mark a region lacking detectable CD31 immunoreactivity. Scale bar: 30 μm. Tissue depth between each stack, 1μm. Total tissue depth, 16 μm.

Supplementary Figure 2

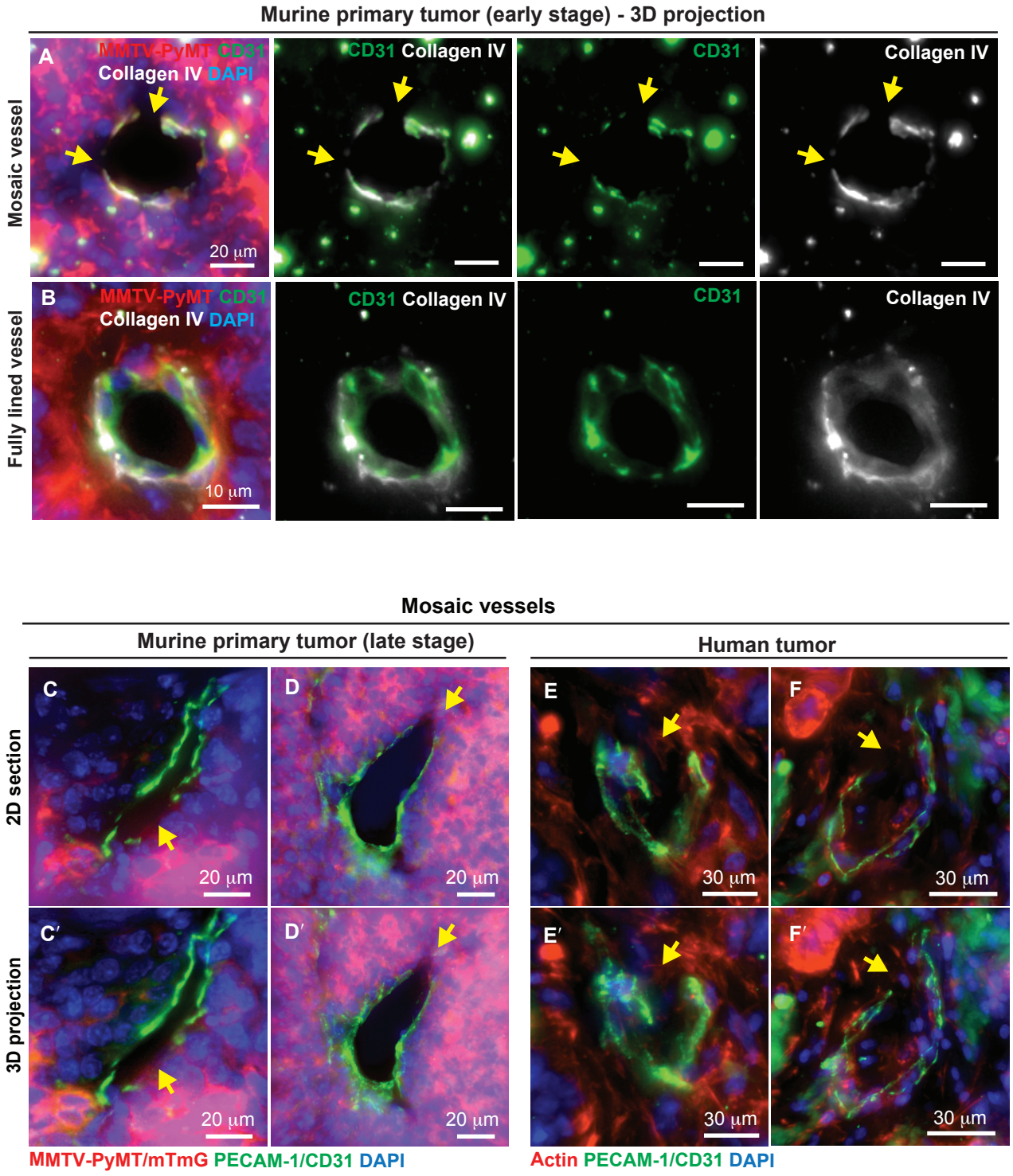

Supplementary Figure 3. Effect of different media conditions on tumor organoid growth within microvessel devices and in 3D organotypic culture.

(A) Representative fluorescence still images of tumor organoids cultured in a microvessel device at Day 1 and Day 3 in culture. Flow is kept at 1 mL/hour and a shear stress of 4 dynes/cm$^{2.}$ The direction of the flow is from left to right of the image. Scale bar: 150 μm. (B) Tumor organoid growth within microvessel devices were evaluated by fold increase in projected surface area of organoids at Day 3 divide by Day 1 in culture with endothelial media (NGM) either without or with 400 μM dibutyryl-cAMP (db-cAMP). n= number of tumor organoids for 2 biological replicates. Error bars indicate s.e.m. P values were determined by the Mann-Whitney test. Differences were considered statistically significant for $p< 0.05$. (C) Representative fluorescence still images of tumor organoids cultured in a microvessel device at Day 1, Day 3 and Day 8 under no flow and shear stress. Scale bar: 100 μm. (D) Schematic representation of 3D organotypic culture of *ROSA^{mTmG}; MMTV-PyMT* tumor organoids using the same culture conditions in the 3D microvessel device. Organoids from the same mouse were culture either with "organoid media" or NGM with or without 400 μM db-cAMP for 5 days. (E-H) Representative still images of tumor organoids for Day 0 (control) and, Day 5 in culture. Scale bar: 50 μm. (I) Tumor organoid growth was evaluated by measuring the projected surface area at Day 0 and Day 5. n= number of tumor organoids, r= 2 biological replicates. Error bars indicate S.D. P values were determined by the ANOVA test. Differences were considered statistically significant for $p< 0.05$. (J) Tumor organoid circularity was determined by calculating the mean circularity score at day 0 and day 5. n= number of tumor organoids, r= 2 biological replicates. Error bars indicate 95% confidence interval. P values were determined by the ANOVA test. Differences were considered statistically significant for $p< 0.05$.

Supplementary Figure 3

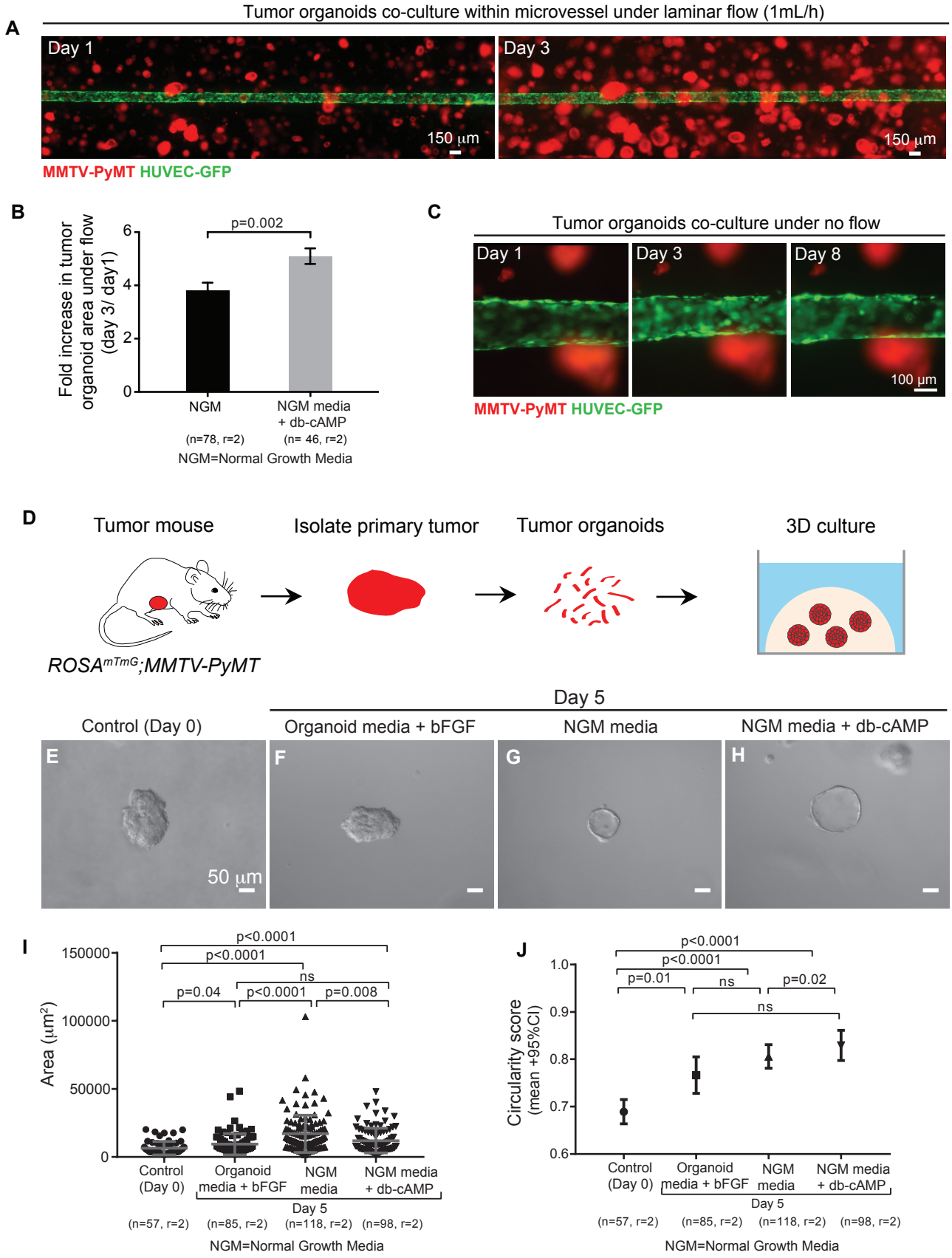

Supplementary Figure 4. Microvessel integrity and functionality in the presence of tumor organoids. Representative fluorescence time series microscopy images of a vessel device cocultured with *ROSAmTmG; MMTV-PyMT* tumor organoids. Permeability was assessed by simultaneously perfusing three different fluorescent molecular weight probes through the vessel lumen: (A-D) 3 kDa dextran (Alexa Flour-488-conjugated), and (F-I) 10 kDa dextran (Alexa Flour-647-conjugated). Time = 0 min represents the frame prior to luminal filling (A'-D' and F'-I') which occurs on average at 20 min. (A"-D" and F"-I") After luminal filing, the fluorescent probes permeate out of the vessel into the ECM. Images and analysis of the other molecular probe in Fig. 3. (E and J) Permeability of 3 kDa and 10 kDa dextran molecular probes increases in the presence of tumor organoids compared to control vessel devices without tumor organoids and decreases when treated with 400 μM dibutyryl-cAMP (db-cAMP) for 24 h. Scale bar: 200 μm. n= number of permeability values calculated for at least 3 biological replicates. Error bars indicate s.e.m. P values were determined by the ANOVA test. Differences were considered statistically significant for $p < 0.05$.

Supplementary Figure 4

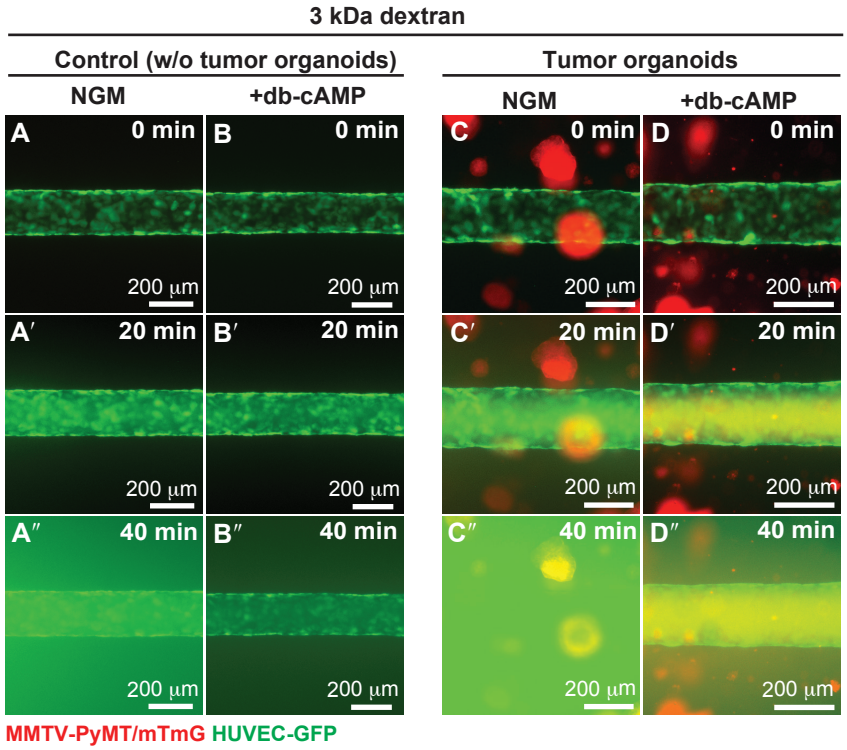

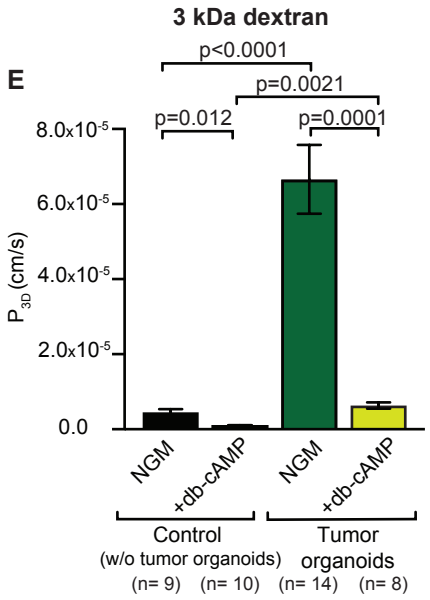

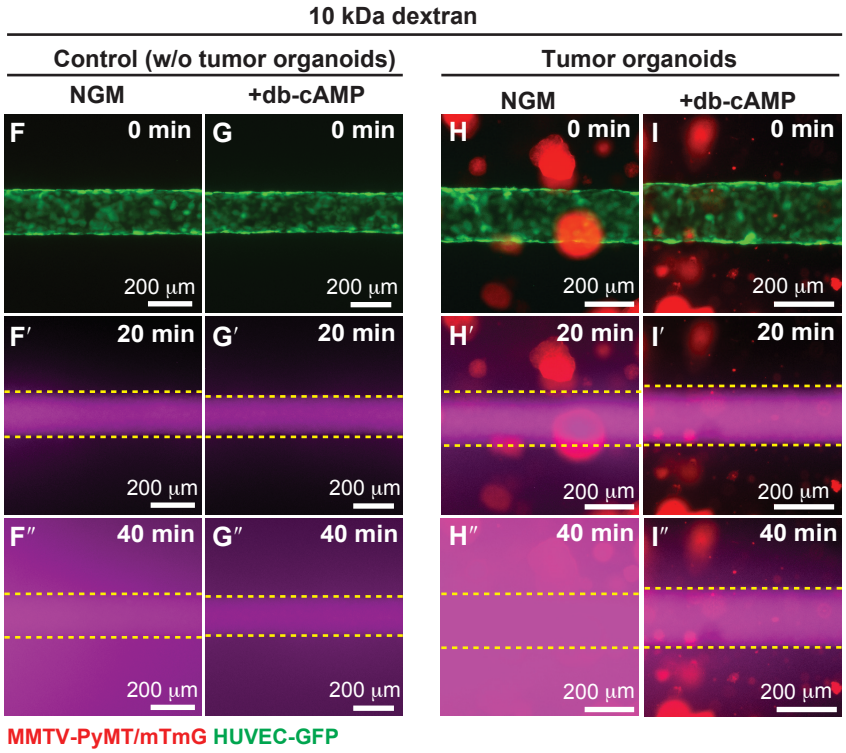

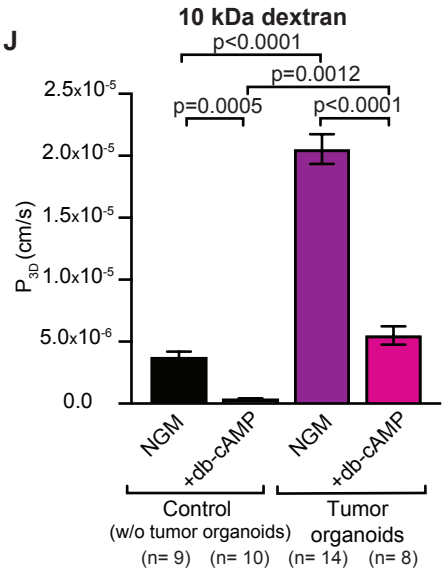

Supplementary Figure 5. Tumor organoids in co-culture with endothelial cells do not express VE-Cadherin. (A) Representative fluorescence microscopy images of a 2D co-culture of *MMTV-PyMT* tumor organoids with endothelial cells (HUVEC-GFP) stained with VE-Cadherin (white) and DAPI. (B) Representative fluorescence microscopy images of a 2D culture of endothelial cells only (HUVEC-GFP) stained with VE-Cadherin (white) and DAPI. (C) Representative fluorescence microscopy images of a 2D culture of *MMTV-PyMT* tumor organoids only stained with Actin (red), VE-Cadherin (white) and DAPI. Scale bar: 50 μm.

Supplementary Figure 5

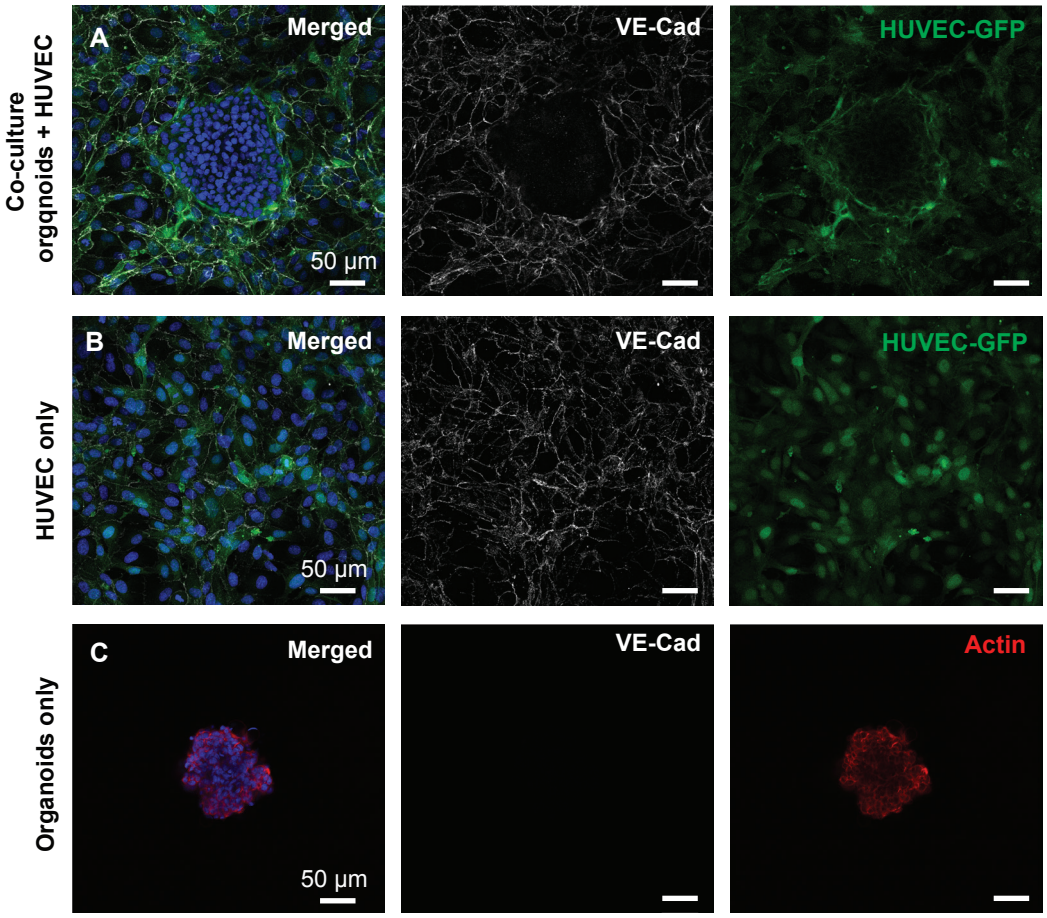

Supplementary Figure 6. Endothelial cell proliferation and cell death within a 3D tumor-microvessel model in the presence of tumor organoids. (A) Schematic illustration of imaging focused at the side view of the microvessel. Individual cell mitosis and death can be visualized and analyzed within the projected endothelium. (B) Representative time-lapse movie of phase-contrast images of an endothelial cell undergoing mitosis. (C) Endothelial cell proliferation rates within the microvessel. (D) Representative time-lapse movie of phase-contrast images of an endothelial cell undergoing cell death. (E) Endothelial cell death rates within the microvessel. Proliferation and cell death rates are reported as %/h. Scale bar: 30 μm, zoom: 20μm. n = number of devices for 3 biological replicates. Error bars indicate s.e.m. P values were determined by the ANOVA test. Differences were considered statistically significant for $p < 0.05$.

Supplementary Figure 6

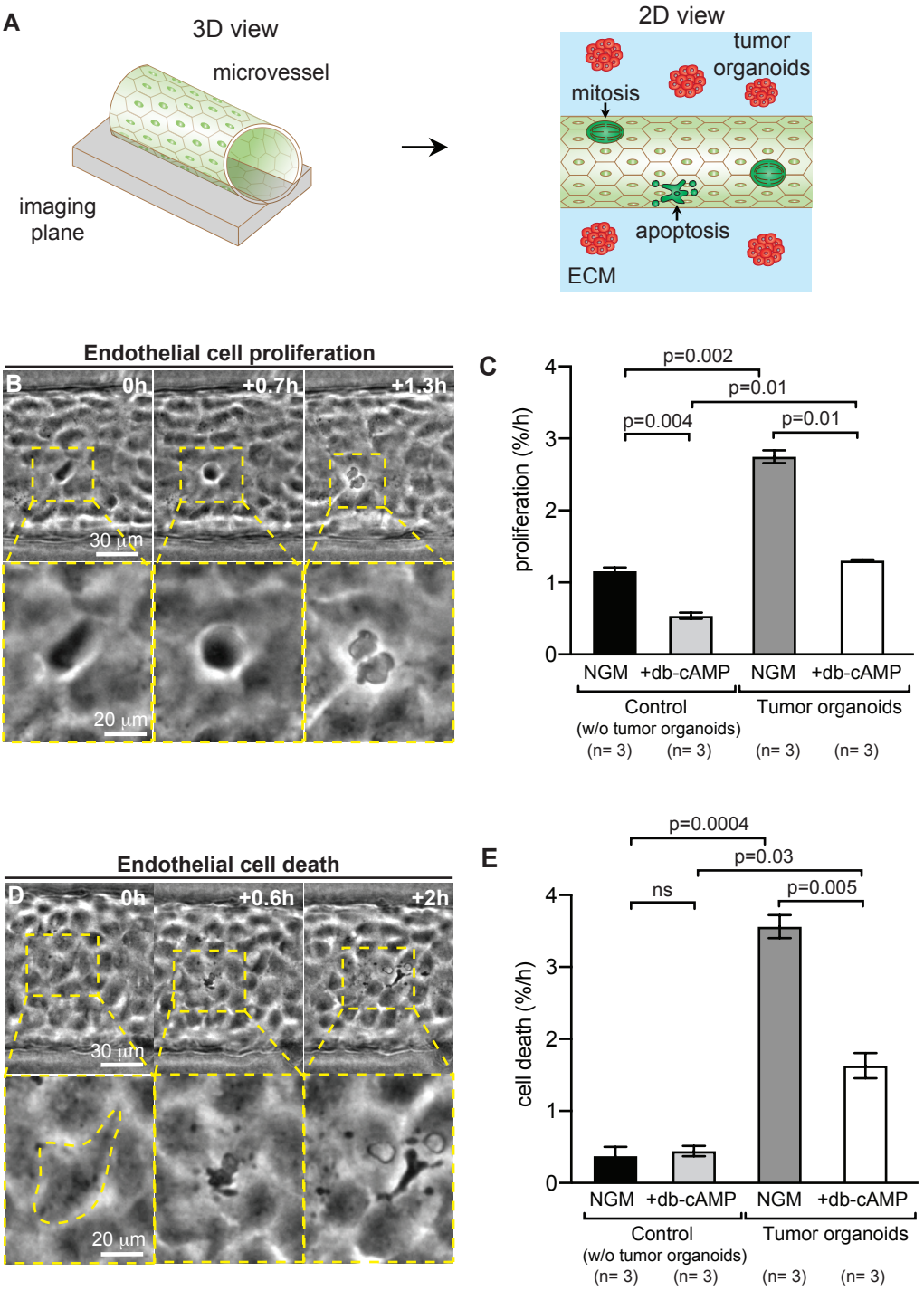

Supplementary Table 1

Table 1. Quantification of mosaic vessels in primary breast cancer tumors.

Tumor	Total no. of vessels	No. of mosaic vessels	% mosaic vessels	Av. mosaic vessel diameter (μm)
Human				
1	246	7	2.8	18.3
2	920	66	7.4	19.2
3	461	30	6.6	15.4
Total	1627	103	Mean 5.6	18.1
			SD 2.4	8.4
Early primary murine (PyMT)				
1	264	19	7.0	35.6
2	341	15	4.0	14.6
3	626	26	4.0	17.6
Total	1213	60	Mean 5.0	22.6
			SD 1.7	16.8
Late primary murine (Orthotopic PyMT)				
1	783	75	9.6	107.4
2	845	43	5.1	91.2
3	1221	50	4.1	76.1
Total	2681	168	Mean 6.3	91.6
			SD 2.9	15.6

Supplementary video S1. Tumor organoids induce transient focal leaks in a tissue-engineered microvessel model. Representative fluorescence time-lapse movie of a microvessel (green) cocultured with *ROSAmTmG; MMTV-PyMT* tumor organoids (red) with poor barrier function showing transient focal leaks to 3kDa dextran (Alexa Flour-488-conjugated, top) and 10 kDa dextran (Alexa Flour-647-conjugated, bottom) probes after luminal vessel filling. These transient leaks are likely due to temporary disruption at cell-cell junctions, which is consistent with a molecular cut off size larger than 3 kDa suggesting paracellular transport. The imaging plane is focused on the vessel equator. Frames were collected every 2 min for 90 min (displayed at 5 frames/s) using a Nikon TE-2000 U microscope (Nikon Instruments Inc., Melville, NY). Flow is kept at 1mL/h and at a shear stress of 4 dynes/cm^2. Flow is from left to right. Scale bar: 200 μm.

Supplementary video S2. Mosaic vessel formation in a 3D tumor-microvessel model. Representative fluorescence and phase contrast time-lapse movie of a *ROSA^{mTmG}; MMTV-PyMT* tumor organoid (red) growing near a microvessel (green). Tumor organoid integrates with the vessel wall forming a mosaic vessel by day 6 in culture. The tumor cells are exposed to the vessel flow which is kept at 1mL/h and at a shear stress of 4 dynes/cm^2. Flow is from left to right. The imaging plane is focused on the vessel equator. Frames were collected every 20 min for 5 days using a Nikon TE-2000 U microscope (Nikon Instruments Inc., Melville, NY). Scale bar: 200 μm.

Supplementary video S3. Vessel barrier function is retained at the site of mosaic vessel formation in a 3D tumor-microvessel model. Representative fluorescence time-lapse movie of a mosaic vessel formed by a *ROSA^{mTmG}; MMTV-PyMT* tumor organoid (red) that integrated with the microvessel wall (green). To analyze barrier function, 3kDa dextran (Alexa Flour-488-conjugated, top) and 10 kDa dextran (Alexa Flour-647-conjugated, bottom) probes were perfused through the microvessel lumen showing retention at the site of tumor-vessel contact. Flow is kept at 1mL/h and at a shear stress of 4 dynes/cm^2. Flow is from left to right. The imaging plane is focused on the vessel equator. Frames were collected every 2 min for 40 min (displayed at 10 frames/s)

using a Nikon TE-2000 U microscope (Nikon Instruments Inc., Melville, NY). Scale bar: 100 μm.

Supplementary video S4. Intravasation event is preceded by mosaic vessel formation. Zoomed in of a representative fluorescence time-lapse movie of a mosaic vessel formed by a *ROSA^{mTmG}; MMTV-PyMT* tumor organoid (red) that integrated with the microvessel wall (green) showing a circulating tumor cell cluster (CTC cluster) being shed into the circulation. The CTC cluster appears to roll on the luminal side of the endothelium as it moves in the direction of flow. Flow is kept at 1mL/h and at a shear stress of 4 dynes/cm^2. Flow is from left to right. The imaging plane is focused on the vessel equator. Frames were collected every 20 min for 5 days (displayed at 7 frames/s) using a Nikon TE-2000 U microscope (Nikon Instruments Inc., Melville, NY). Scale bar: 100 μm.

Supplementary video S5. Mosaic vessel formation using a parallel tumor-vessel arrangement in a tissue-engineered microvessel model. Representative fluorescence time-lapse movie of a *ROSA^{mTmG}; MMTV-PyMT* tumor (red) sending invasive collective strands growing in the direction of the microvessel (green). Tumor strand integrates with the vessel wall forming a mosaic vessel. The tumor cells are exposed to the vessel flow which is kept at 1 mL/h and at a shear stress of 4 dynes/cm^2. Flow is from left to right. The imaging plane is focused on the vessel equator. Frames were collected every 20 min for 3 days (displayed at 12 frames/s) using a Nikon TE-2000 U microscope (Nikon Instruments Inc., Melville, NY). Scale bar: 50 μm.